

2018

## The N-acyltransferase Lnt: Structure-function insights from recent simultaneous studies

Wei Chang

Declan A. Doyle

Toufic El Arnaout

Follow this and additional works at: <https://arrow.tudublin.ie/schfsehart>



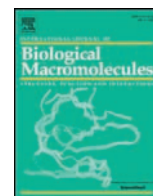
Part of the [Food Science Commons](#), and the [Medicine and Health Sciences Commons](#)

---

This Article is brought to you for free and open access by the School of Food Science and Environmental Health at ARROW@TU Dublin. It has been accepted for inclusion in Articles by an authorized administrator of ARROW@TU Dublin. For more information, please contact [arrow.admin@tudublin.ie](mailto:arrow.admin@tudublin.ie), [aisling.coyne@tudublin.ie](mailto:aisling.coyne@tudublin.ie), [gerard.connolly@tudublin.ie](mailto:gerard.connolly@tudublin.ie).



This work is licensed under a [Creative Commons Attribution-NonCommercial-Share Alike 4.0 License](#)



## Review

## The N-acyltransferase Lnt: Structure-function insights from recent simultaneous studies

Wei Cheng<sup>a</sup>, Declan A. Doyle<sup>b</sup>, Toufic El Arnaout<sup>c,\*</sup><sup>a</sup> Division of Respiratory and Critical Care Medicine, State Key Laboratory of Biotherapy, West China Hospital of Sichuan University and Collaborative Innovation Center of Biotherapy, Chengdu, Sichuan 610041, China<sup>b</sup> Biological Sciences, University of Southampton, Southampton SO17 1BJ, UK<sup>c</sup> School of Food Science and Environmental Health, Dublin Institute of Technology, Marlborough St, Dublin 1, Ireland

## ARTICLE INFO

## Article history:

Received 22 January 2018

Received in revised form 29 May 2018

Accepted 30 May 2018

Available online 31 May 2018

## Keywords:

Lipoproteins

Acyltransferase

Nitrilase

## ABSTRACT

Bacterial lipoproteins have been researched for decades due to their roles in a large number of biological functions. There were no structures of their main three membrane processing enzymes, until 2016 for Lgt and LspA, and then 2017 for Lnt with not one but three simultaneous, independent publications. We have analyzed the recent findings for this apolipoprotein N-acyltransferase Lnt, with comparisons between the novel structures, and with soluble nitrilases, to determine the significance of unique features in terms of substrate's recognition and binding mechanism influenced by exclusive residues, two transmembrane helices, and a flexible loop.

© 2018 Elsevier B.V. All rights reserved.

## Contents

1. An introduction on bacterial lipoprotein processing. . . . .	870
2. Lnt as a nitrilase. . . . .	872
3. The recent crystal structures of Lnt . . . . .	873
4. The access to the active site of Lnt . . . . .	876
4.1. The long flexible loop . . . . .	876
4.2. E343 as an important and fixed residue. . . . .	876
4.3. Is F82 a gatekeeper? . . . . .	876
4.4. Lessons from soluble nitrilases . . . . .	876
Acknowledgements . . . . .	876
References. . . . .	876

## 1. An introduction on bacterial lipoprotein processing

Three membrane proteins are involved in processing precursors of lipoproteins, in the following order: the diacylglycerol transferase Lgt, the signal peptidase LspA, and the N-acyltransferase Lnt (structures in Fig. 1) [1–5].

Lgt transfers a diacylglycerol to a conserved cysteine connected to a signal peptide at its N-terminus. Lgt contains important residues identified such as R143/R239 (highly conserved) and H103/Y235 (less

conserved) (large and small spheres in Fig. 1, respectively). It also has two clefts [1]: the front cleft for the entrance of phosphatidylglycerol (PG) through transmembrane helices (TMHs) 1 and 2, and the side cleft through TMHs 3 and 7 for the pre-prolipoprotein containing the lipobox.

The modification by Lgt is required for LspA's activity on prolipoproteins [7, 8] to cleave the signal peptide, with certain exceptions as observed in the Gram-positive bacterium *Listeria monocytogenes* [9]. LspA, also known as Lsp, SPase II or type II signal peptidase, employs Asp124 and Asp143 as catalytic residues, and the TMHs at which the substrate binds seem to be TMHs 2 and 4. LspA is generally essential in Gram-negative bacteria but not in Gram-positive

\* Corresponding author.

E-mail address: [toufic.elarnaout@dit.ie](mailto:toufic.elarnaout@dit.ie) (T. El Arnaout).

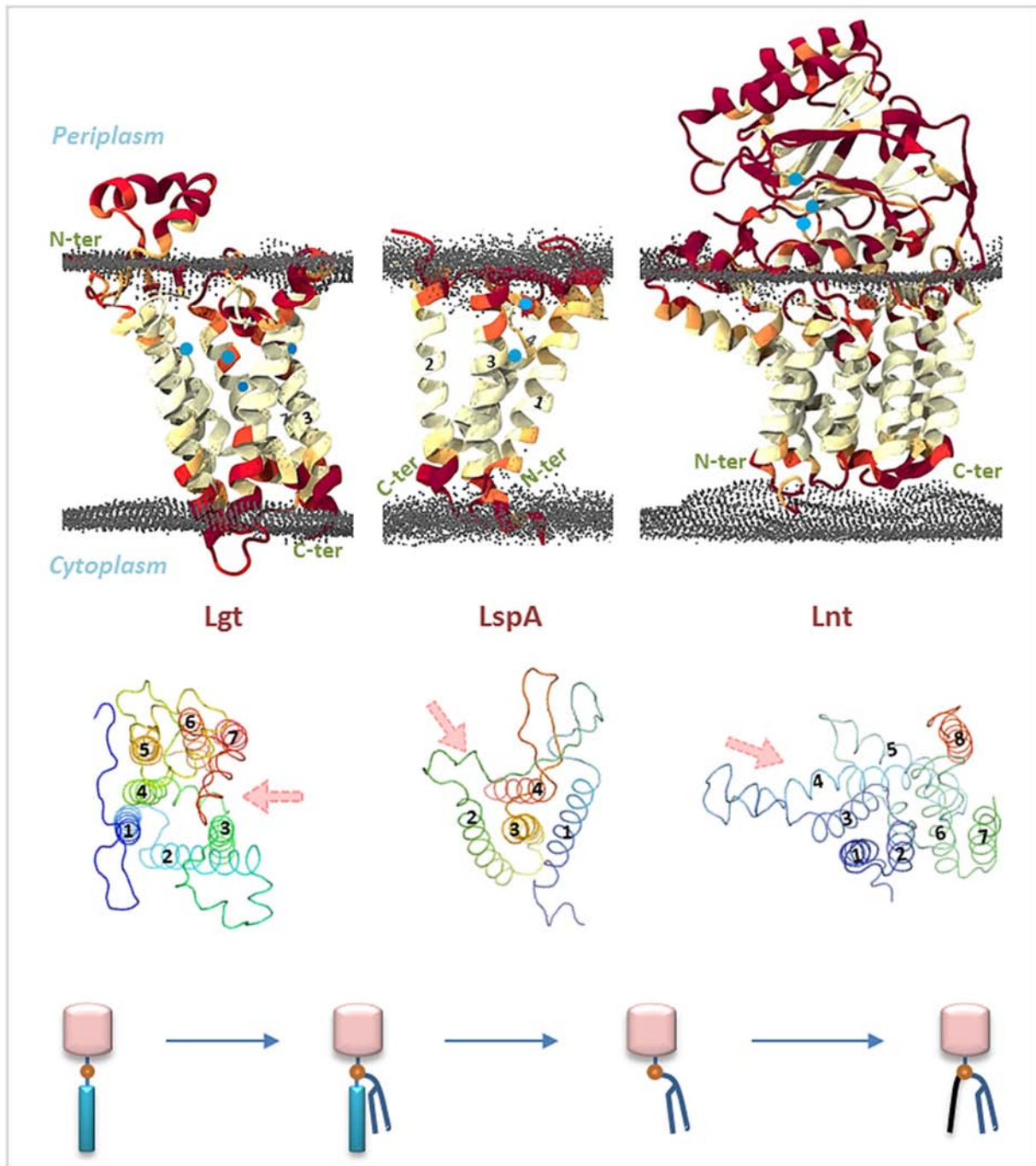


**Fig. 1.** The crystal structures of the lipoprotein processing enzymes Lgt, LspA and Lnt. (left) Lgt, PDB ID 5AZC [1]; (middle) LspA, PDB ID 5DIR [2]; (right) Lnt, PDB ID 5VRG [3]. Top row: Pre-rendered cartoon representations in VMD using Tachyon and showing contacts (“average occupancy within 6 Å of the protein over the final 800 ns of simulation time”) between solvent and protein, obtained using MemProtMD [6]. Details manually drawn are selected important residues (blue spheres). Middle row: Ribbon representations using PyMOL with TMH numbers of the structures viewed from the top (only the TM domain is shown for Lnt). The arrows indicate the likely binding sides of the pre-prolipoprotein, prolipoprotein and apolipoprotein in Lgt, LspA and Lnt, respectively. Bottom row: Illustrations of the lipoprotein modifications at each step.

bacteria [10, 11]. Other proteases can process the lipoprotein precursors in Gram-positive bacteria for mature lipoprotein secretion but are poorly known or identified [12].

The third step is the action by Lnt on apolipoproteins. It catalyzes the transfer of an acyl chain from the *sn*-1 position of a lipid to the N-ter cysteine, generating a triacylated lipoprotein. In its structure, a catalytic triad (E267/K335/C387) is accessible near TMHs 3, 4 and 5, and a long and unique loop (also described as an arm, lid, etc.) containing a short helix. It is possible that the acyltransferase activity varies depending on the membrane's composition and availability of lipids. In the cell

envelope of *E. coli*, *in vitro/vivo* studies have indicated that any major phospholipid (phosphatidylethanolamine, phosphatidylglycerol, cardiolipin) can serve as an acyl donor [13, 14] (with a certain order of preference). Furthermore, Lnt is generally essential in Gram-negative bacteria [15, 16] except in some species [17], and absent in most Gram-positive bacteria. However, Lnt homologs may be present in Gram-positive bacteria of complex cell envelope [18, 19]. In some Gram-positive species, Lnt may be possibly found in GC-rich (*i.e.*, high G + C content) [20–22] but not in low GC content bacteria, even though the last step (*i.e.*, becoming triacylated) has been observed [23, 24].

Furthermore, a different gene (named *lit*) in low GC content Gram-positive bacteria is associated with the function of lipoprotein 'intramolecular transacylation' (using Lit, a smaller protein than Lnt) for forming N-acylated lyso-form lipoproteins [25, 26].

## 2. Lnt as a nitrilase

The Nitrilase superfamily comprises proteins with important functions (e.g., nitrilases, amidases, carbamylases). Characterization may be necessary to validate the nitrilase classification (e.g., an amidase [27]). It has been suggested that Lnt is a reverse amidase and belongs to the Nitrilase superfamily (branch #9) [28]. On top of Lnt's transmembrane (TM) domain sits the nitrilase (Nit) domain (Figs. 1 and 2). Nitrilases generally require the Glu/Lys/Cys catalytic triad's conformation, also found in Lnt, and have a conserved  $\alpha\beta\beta\alpha$  sandwich fold. Many nitrilases exist in an oligomeric state, in which generally the bottom large surface under the active site is involved in the assembly (in Lnt, this surface sits on the TM domain (Figs. 1 and 2)). The similarity of a major domain of Lnt to soluble nitrilases may make it difficult to discover unique and novel antibiotics, unlike LspA which is more unique in structure and species exclusivity for example, in order to combat virulence caused by lipoproteins [29]. In the three recent crystal structure publications of Lnt, the classification of Lnt was focused on the broad Hydrolase superclass [3] with the Nitrilase term mentioned once, but more often revolved around the 'Nitrilase' principle in [4, 5], even though all three studies identified the sandwich and triad features.

The structure of Lnt was described to have a significant shortening in regions ' $\beta 2$  to  $\alpha 2$ ', and ' $\beta 9$  to  $\beta 10$ ', compared to other nitrilases [5]. The general base was also proposed to be E267 which activates the nucleophile C387. During the transacylation reaction a thiol-acyl intermediate is formed. The oxyanion hole is partly facilitated by K335 for stabilizing the tetrahedral intermediate.

In reality, in Lnt the full reaction occurs as a two-step mechanism known as ping-pong which was also described [3–5]. First, the intermediate is formed by the nucleophilic attack on the *sn*-1-glycerophospholipid's carbonyl (in phosphatidylethanolamine (PE), preferentially). Second, the intermediate (acyl-Lnt) undergoes a nucleophilic attack by the  $\alpha$ -amino group of the protein substrate generating the triacylated lipoprotein [3]. Looking at one of the several other types of acyltransferases for varying biological functions [34], the DHHC (Asp-His-His-Cys) enzymes which are protein acyltransferases (i.e., palmitoyltransferases, PATs) also function using a two-step mechanism [35, 36]. These are eukaryotic integral membrane enzymes that catalyze protein S-acylation using a nucleophilic cysteine. Structures of DHHC enzymes were recently determined [37], including that of a covalent intermediate mimic. The authors described candidate cysteines for palmitoylation proximal to the membrane, and an enzyme's active site with a catalytic triad-like arrangement. Aromatic amino acids in/at the acyl binding cavity were also analyzed due to important roles, such as Tyr181, which when mutated to an alanine it changes the enzyme's preference from C16 to C18. Such acyl chain selectivity was also observed in another family based on the structure of PlsC, a 1-acyl-*sn*-

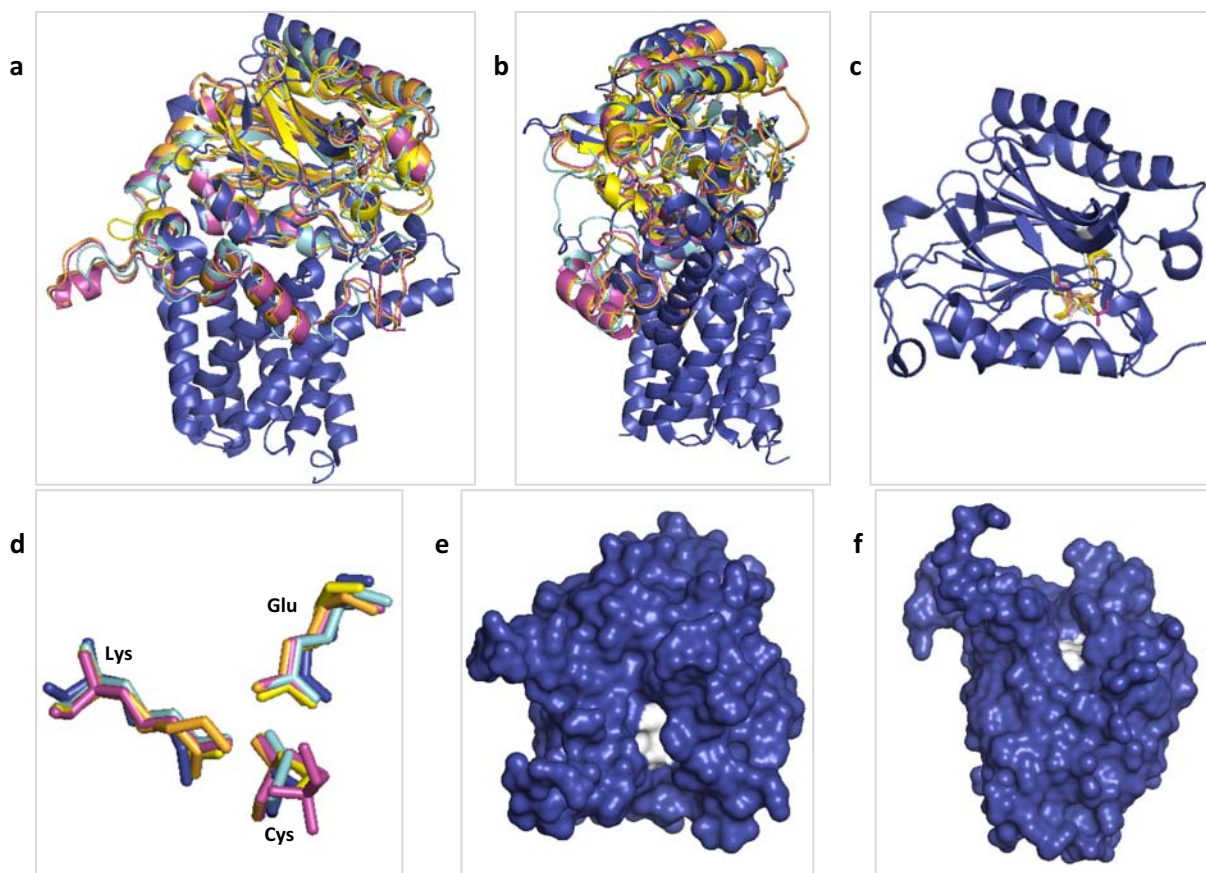


**Fig. 2.** Structural comparison of Lnt to soluble nitrilases. a and b: Front view of the superimposition and side view facing the active site, respectively. The chosen PDBs are the following: 5VRG (blue, Lnt, triad E267-K335-C387) [3]; 2DYU (cyan, the formamidase AmiF, triad E60-K133-C166) [30]; 4LF0 (orange, an amidase, triad E59-K134-C166) [31]; 3IVZ (yellow, the thermoactive nitrilase PaNit, triad E42-K113-C146) [32]; and 2UXY (magenta, an amidase, triad E59-K134-C166) [33]. c: Front view of the Nit domain of Lnt, with all triads superimposed. d: A closer look at the triad positions shown in sticks. Note that Cys in 2UXY and 3IVZ are in other states (C3Y/CSX). e and f: Surface representations of the side view facing the binding cavity, and from the bottom, respectively, with the triad colored in white. Figures were generated using PyMOL.



glycero-3-phosphate (LPA) acyltransferase (called LPAAT) [38] which is membrane-anchored. Its 16:0 preference was changed to 14:0 in the G25M mutant construct.

For PaNit which is another nitrilase (triad E42-K113-C146) (Fig. 2) it was proposed that the nucleophile is Cys, the general base is Glu [39], the general acid is Lys/Glu, an ordered H<sub>2</sub>O is a hydrolytic water, and the oxyanion hole is formed by N<sub>ζ</sub>-Lys113 and N<sub>ζ</sub>-Phe147 [32]. Particularly in Lnt, an additional residue, Glu343 (Section 4.2) that is positioned close to the triad, conserved in Lnt homologs but not in the Nitrilase superfamily, was identified as very important for the reaction and for stabilizing Lys335 [3, 5]. Furthermore, notice that in PaNit, Phe147 is beside Cys146. In Lnt, Tyr388, previously shown as essential [40], is in such position following Cys387. However, the Y388F mutation maintains similar growth unlike Y388A [3]. Furthermore, the Y388W construct (inactive) [5] is able to form the acyl-enzyme intermediate, therefore not disrupting the first step during the ping-pong mechanism. Our analysis of all five *E. coli* Lnt PDBs (Protein Data Bank) deposited showed that Tyr388 aligns well in PDB IDs 5N6H, 5N6L, 5VRH and 5XHQ, but is slightly rotated in 5VRG (by 2.7 Å at the phenolic OH-group). However, its distance to G145 (conserved residue) remains a little similar as in PDB ID 5XHQ and 5VRH (this distance is shorter in PDB ID 5N6H and longer in PDB ID 5N6L). Close to it (in PDB 5VRG) is palmitic acid (PLM) bound, while in 5N6L (mutant) and 5VRH (mutant) it is a monoolein (OLC) molecule (Fig. 4.c) (all three PDBs contain bound lipids). As a wild-type (WT) structure, 5VRG provides great insight of Tyr388 movement based on the lipid architecture, compared to the other WT structures (5XHQ and 5N6H). Tyr388 may likely contribute to pocket hydrophobicity for lipid binding as well as Van der Waals interactions with the acyl of the intermediate [3], and the other study [5]

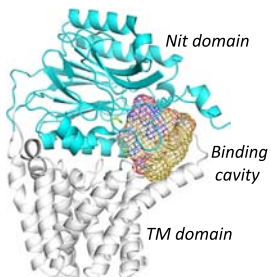
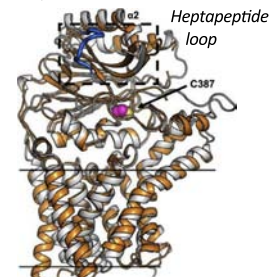

suggested a role in the 2nd step related to the binding of the protein substrate.

### 3. The recent crystal structures of Lnt

Several approaches, some in common, were employed in the simultaneous structure-function studies of Lnt (Table 1). They all reported a structure with a TM domain of eight TMHs and a Nit domain. The structure contains 7 TMHs + 1 C-ter TMH, with a clear answer to previous experiments that used the PhoA/LacZ reporter method [41]. The studies also presented models of the Lnt-acyl intermediate. We found the PDBs of structures to superimpose with high TM-scores [42]: 0.97 for 5N6H vs 5XHQ, 0.98 for 5N6H vs 5VRG, and 0.95 for 5XHQ vs 5VRG [3–5]. While the three studies solved the structure of *E. coli* Lnt, the structure of *Pseudomonas aeruginosa* Lnt (LntPae) was also solved [4], with one main highlighted difference which is the absence of a 325–331 YSYESAD motif (indicated in Table 1) found in *E. coli* Lnt and of no clear role.

A mutation of Cys387 to a Serine in Lnt can form an intermediate that is resistant to neutral hydroxylamine treatment [43]. However, the C387S mutant has modest [3] or no activity [4] compared to the WT, and also the C387A mutant (does not form an acyl intermediate) is inactive [43]. Indeed, attempts were pursued to solve the structure of a C387S construct [3, 4] which were successful in one study (PDB ID 5VRH) [3]. However, it appeared that the lipid revealed was not covalently bound. Such a structure contained two lipids located inside the cavity (similarly to the WT structure, PDB ID 5VRG), with a F82 residue fully closed behind (Fig. 3.c and d). This residue has different positions in the other PDBs, even in PDB ID 5N6L (C387A) [4] which also has two similar lipids bound in the cavity, probably due to another two

**Table 1**  
Brief comparison of the three studies on the N-acyltransferase (Lnt).

	Lu et al. [5]	Wiktor et al. [4]	Noland et al. [3]
Structures solved	<i>E. coli</i> Lnt WT	<i>E. coli</i> Lnt WT, <i>E. coli</i> Lnt C387A, <i>P. aeruginosa</i> Lnt WT	<i>E. coli</i> Lnt WT, <i>E. coli</i> Lnt C387S
PDB IDs	5XHQ	5N6H, 5N6L, 5N6M	5VRG, 5VRH
Resolution(s)	2.59 Å	2.9, 2.9 and 3.1 Å	2.52 and 2.14 Å
Structure			
Assays	(from figure 2.e of [5]) Alkylation assay with maleimide-PEG and SDS-PAGE with immunoblotting of Lnt and Lnt-malPEG. Transacylation assay using FSL-1, lipids and SDS-PAGE. Mass spectroscopy. Thermostability assay. <i>In vivo</i> complementation activity assay.	(from supp. figure 11.a. of [4]) TLC on NBD-PE and NBD-lyso-PE. SDS-PAGE and Western-blot of FSL-1-biotin with(out) N-acylation.	(from figure S3.A. of [3]) Substrate peptide Pam2Cys-peptide-biotin and lipids, with Western-blot and mass spectrometry. Complementation studies. <i>In vivo</i> infection and serum sensitivity assays.
Molecular dynamics simulations	Lipid bilayer (DPPE and DPPG)	Lipid bilayer (POPG and POPE)	Lipid bilayer (POPE)
Crystallization method	Vapor-diffusion	Lipidic cubic phase	Lipidic cubic phase
Detergents	DM for solubilization. NTM for final purification.	LMNG for solubilization and final purification.	DDM for solubilization and final purification.
Protein concentration	12 mg/mL	13 mg/mL	40 mg/mL
Synchrotron(s)	Shanghai Synchrotron Radiation Facility (SSRF, China); Spring 8 (Japan); Photon Factory (KEK, Japan)	Swiss Light Source (SLS, Switzerland)	Advanced Photon Source (APS, USA); Advanced Light Source (ALS, USA)
Lipids in the binding cavity	Refer to Fig. 3.d and Fig. 4.a		

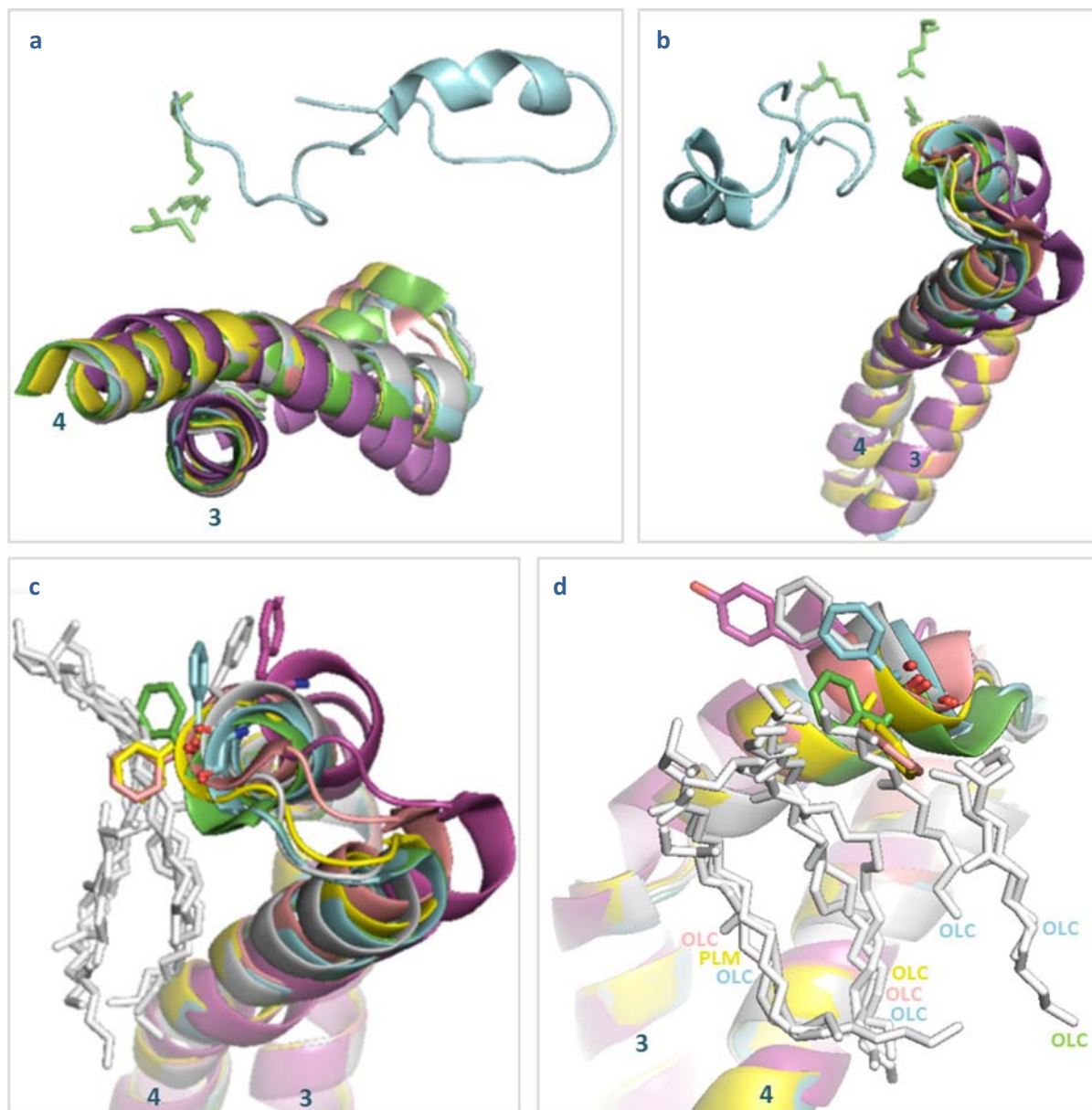


**Fig. 3.** Positions of the long flexible loop and F82 relative to the active triad in Lnt. Structural coordinates were used from *E. coli* Lnt PDB IDs 5N6H (green), 5N6L (cyan, C387A), 5VRG (yellow), 5VRH (pink, C387S) and 5XHQ (grey). *P. aeruginosa* Lnt is in magenta (PDB ID 5N6M). The two helices are TMHs 3 and 4. The active triad is shown in green sticks in 'a' and 'b'. a: View from the bottom. b: Side view facing the active site as in Fig. 2.b and c. c: View of TMHs 3 and 4, F82 positions (Y80 in *P. aeruginosa* Lnt), as well as the lipids (grey sticks) found in some PDBs. d: Front view as in Fig. 2.a and c showing the positions of F82 (Y80 in *P. aeruginosa* Lnt), and lipids labelled using colors corresponding to the PDB ID of origin (pink, yellow, cyan, green). Figures were generated using PyMOL.

additional, succeeding lipids behind (with one occupying the path of F82) (Figs. 3.d and 4.a). Furthermore, in PDB ID 5VRH (C387S), the OLC lipids in positions 1 and 2 appear ~6 Å higher towards the triad than in 5N6L (C387A) (Fig. 4.a and c). The latter shows no relevant interaction of an OLC in the PDBsum/Ligplot [44].

The coordination of closely bound lipids in the C387S structure (PDB ID 5VRH) guided in the proposal of a potential POPE (1-palmitoyl-2-oleoyl-phosphatidylethanolamine) binding model [3]. As described in Section 2, upon binding, the *sn*-1-acyl chain carbonyl undergoes a nucleophilic attack by C387. S-palmitoyl-Lnt intermediate is formed and the lyso-PE is released. The next step is the N-acylation of the lipoprotein: an acyl chain of a S-diacylated lipoprotein binds positioning the N-ter S-diacylglyceryl-cysteine of the lipoprotein for nucleophilic attack

on the S-palmitoyl-cysteine in Lnt. The resulting triacylated lipoprotein is then released.

Near the active site, a putative phosphate recognition site was also exclusively proposed [3] based on a chloride ion (Fig. 4.a) and its coordination by several residues among which is the generally essential and conserved W237 [3, 40, 43, 45]. In total, the PDBsum/Ligplot of interactions [44] shows interactions of the chloride ion with Asn412, Trp237, Lys236 and Trp415 (PDB ID 5VRH), and with Asn412 and Trp237 (PDB ID 5VRG). It might be a binding site of the negatively charged phosphate part of the head group of POPE, and/or an ion coordination site important for the protein stability. In other proteins, there are examples of hypothesis that conserved residues coordinating a  $\text{SO}_4^{2-}$  ion are the ones that coordinate the phosphate of inositol phosphate

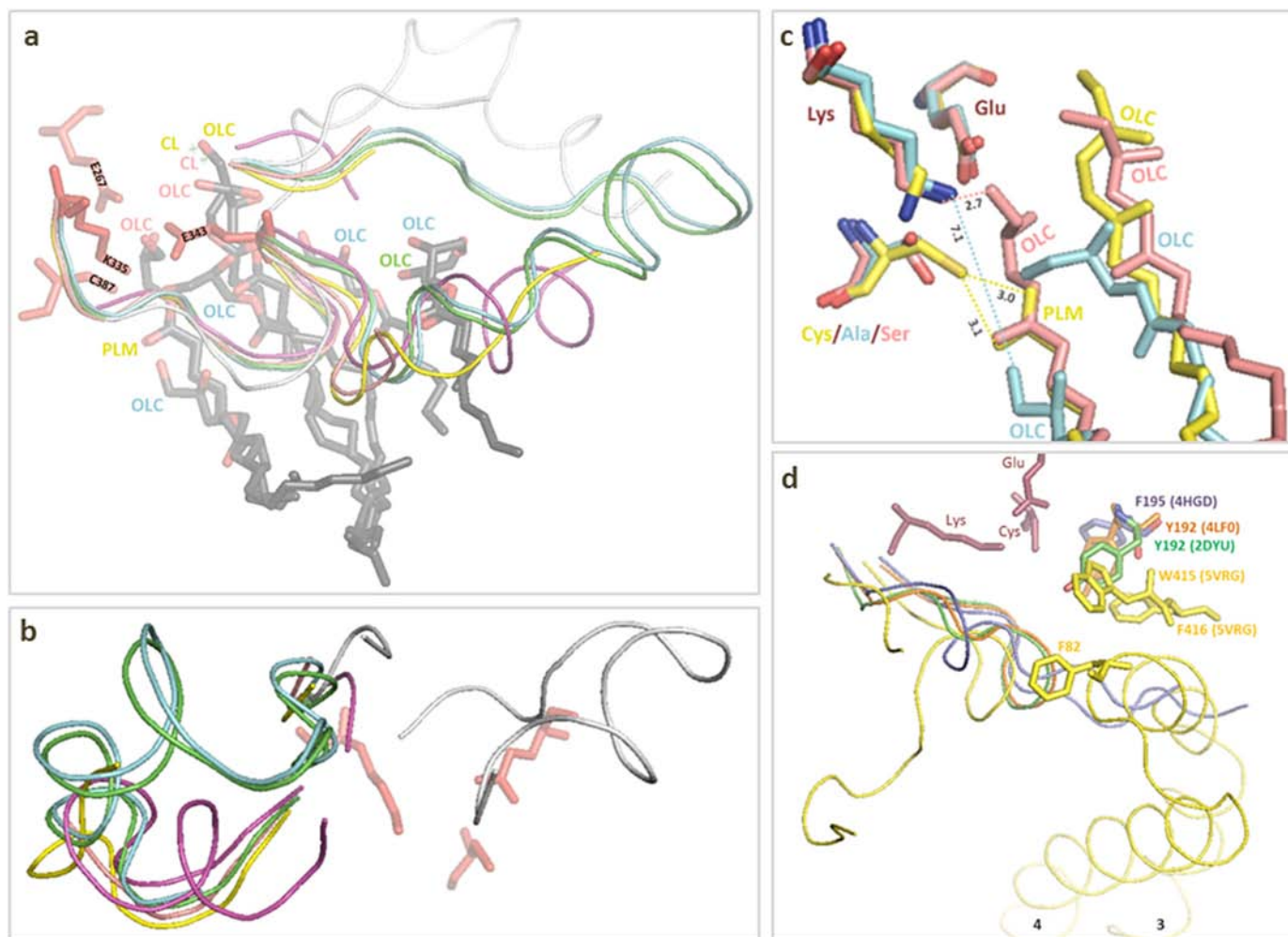


**Fig. 4.** Comparison of structural features at the binding cavity in Lnt. PDB IDs are *E. coli* Lnt 5N6H (green), 5N6L (cyan, C387A), 5VRG (yellow), 5VRH (pink, C387S) and 5XHQ (grey). *P. aeruginosa* Lnt is in magenta (5N6M). a: Front view as in Fig. 2.a and c and Fig. 3.d showing the active triad and flexible loop. The triad E267/K335/C387 generally superimposes well and is shown as red sticks. The position of E343 is also shown. Selected protein features include the long flexible loop (cyan in Fig. 3), starting from residues after K335 and until F365. Part of the loop is incomplete in several structures. All bound molecules are also shown in black sticks and labelled with colors according to the corresponding PDB ID. b: Side view facing the binding cavity as in Fig. 2.b and 3.b. c: Triad H-bonding interactions between Cys-PLM in 5VRG (yellow), Lys-OLC in 5VRH (pink, C387S), or otherwise the distance Lys-OLC in 5N6L (cyan, C387A). d: View towards the binding site in Lnt compared to soluble nitrilases showing the differences in loops. TMHs 3 and 4 are shown for Lnt. PDB IDs employed are 5VRG (Lnt WT, yellow) [3], 2DYU (formamidase AmiF, green) [30], 4HGD (Nit2 C169S solved in complex with a ligand, blue) [49], and 4LF0 (amidase E142D, orange) [31]. Alignments may slightly vary based on the macromolecule of reference. Figures were generated using PyMOL.



[46]. Furthermore, some nitrilases were found to be likely dependent of certain metal ions (like  $\text{Co}^{2+}$  although it is positively charged [47]), but other nitrilases do not require divalent ions [48].

#### 4. The access to the active site of Lnt

##### 4.1. The long flexible loop

The sequence from K335 to C387 (Nit domain) is of particular interest because K335 and C387 are involved in the catalytic triad (with E267), E343 is very important for the triad, and a large part of this sequence represents a long loop containing a short helix and a lid loop that is flexible, amphipathic, formed by residues F357–Q372 [5] (Fig. 3.a and b). The latter study also carried out molecular dynamics (MD) simulations and it seems that the lid loop strongly interacts with the membrane. Based on the analysis of the sequence, including the long loop and fixed residue E343 in the next Section, the parts of largest flexibility are F344 to S363, and slightly V339 to G342. In the structure solved using crystals grown by vapor diffusion (PDB ID 5XHQ) [5], the lid is significantly higher than in those solved using crystals grown by the lipidic cubic phase (LCP) method (Fig. 4.a and b). Furthermore, the previous hypothesis based on the Sortase mechanism involving loops (e.g., opening, closing, substrate recognition) [45] was not mentioned in the three studies.

The active triad generally superimposes in all PDBs analyzed, but not this loop, which in several cases is not ordered or partly invisible in the structures (Fig. 4.a and b), and in certain PDBs where it was found complete, only one of the two chains in such PDBs displayed such a full loop. Located in the space between the long loop and TMHs 3 and 4 (Fig. 3.c and d) is the F82 residue hypothesized as a gate residue towards the binding groove [3], discussed in Section 4.3.

##### 4.2. E343 as an important and fixed residue

This amino acid is included in the sequence K335 to C387 highlighted above. Surprisingly, our analysis of the crystal structures (Fig. 4.a and b) shows that this residue overlaps very well (only  $\sim 1.5$  Å lower in PDB ID 5XHQ), even when the loops significantly diverge afterwards (F344 to S363) in each PDB ( $\sim 20$  Å higher at L347 in PDB ID 5XHQ), or slightly prior to it (V339 to G342). The position of E343 is close to the triad (Fig. 4.a). It is essential for the function, and important for the reaction particularly for K335 and the stability of intermediates [3, 5]. A role with E267 in the activation of C387 was also discussed [43]. It is well conserved in Lnt homologs. Its role was suggested in the first step of the reaction based on the E343A mutation [5]. Furthermore, another role E343 may have was also suggested in the binding of substrates due to an interaction with the second bound lipid (OLC) in PDB ID 5VRH [3] (Fig. 4.a and c).

##### 4.3. Is F82 a gatekeeper?

Its possible purpose was specified in lipid binding and release, permitting the enzyme to encircle the bound lipids (Fig. 3.c and d) in an induced-fit mechanism before attack by C387 [3]. Therefore, following binding, F82 closes and the S-palmitoyl-Lnt intermediate is formed. When it opens, the lyso-PE is released. The authors also provided 'gate' poses using MD simulations, and highlighted a potential role for F341 right opposite to it, part of the region of low flexibility (V339–G342), prior to the most flexible part (F344–S363) of the long loop.

In the other PDB IDs we analyzed (Fig. 3.c and d), 5VRH and 5VRG each contains two lipid molecules in the binding pocket, with F82 found in the closed (low) position and superimposing well. In 5N6H there are two chains: the first protein chain has a fully visible long loop, one OLC lipid bound outside the cavity, and with F82 half way through, while the second chain (not shown here) has a partially visible loop, no bound lipids in or around the cavity, and with F82 rather more

raised ( $5.4$  Å) towards a position similar to that in PDB ID 5XHQ. In 5N6M (*P. aeruginosa* Lnt) which has an unoccupied active site, the corresponding residue (Y80) is fully open. In the 5N6L mutant, the site contains two lipid molecules as well as an additional two molecules behind, one occupying F82's path and the last one further back in the position of the exterior OLC in 5N6H. In 5XHQ, the long loop (mostly the short helix) is fully raised as well as F82, with no lipids bound (like 5N6M).

Therefore, it appears difficult to robustly conclude the relation between F82's position, the long flexible loop (raised vs lowered), and an induced-fit model mechanism. Indeed, while F82 was suggested as important for positioning the lipids [3], the authors also found that F82 (and F341) mutants provided normal growth, possibly that the gating hypothesis is weak and F82 does not impact on the lipid affinity, but its absence may even increase the efficiency.

##### 4.4. Lessons from soluble nitrilases

The analysis of the loop region features (Fig. 4.d) revealed that several soluble nitrilases have a loop that is shorter in length and more ordered. The overall structures of these nitrilases overlap with the nitrilase part of Lnt, as observed for PDB IDs 4LFO and 2DYU (an amidase and formamidase [30, 31]) (Fig. 2). In PDB ID 4HGD (yeast Nit2 C169S with a ligand [49]), this loop is longer than the loops in 4LFO and 2DYU, and extends to an angle close to F82's position at the top of TMHs 3 and 4 in Lnt. Apart from the triads that also align well, some of the soluble nitrilases may exhibit surface features (and total sequence) that are significantly smaller or larger in size and/or are characterized by an oligomeric state. The loops may also impact on the exposure to substrates and solvents and control the binding volume. The sequences can be also very dissimilar [5]. In Lnt, the TM/Nit architecture together with the loop flexibility permit a lateral access from the membrane for apolipoproteins as well as lipids. Furthermore, one may assume, if the conformation of the loop in the high position in PDB ID 5XHQ was ignored, that the loop may be maintained in the low position (as in Fig. 3.b) at all times, with the binding of substrates occurring straight-forward between the loop and TMHs 3–4. It is also possible that the loop changes from the high to the low position (Fig. 4.a and b) due to the interaction with the membrane and while the lipid (with the acyl chains and head group) is accessing into the cavity, but it is difficult to draw a conclusion as certain structures do not contain internally bound lipids but still showed a loop in the low position, unless this was caused by certain factors such as the LCP crystallization method. As for F82 as a (mostly unlikely) potential gate residue in Lnt (Section 4.3), since soluble nitrilases do not contain the TMHs 3 and 4 found in Lnt, we were unable to identify a residue similar in position to F82. In fact, the analyzed soluble nitrilases have closer residues, Y192/Y192/F195 at the binding pockets (Fig. 4.d) (more complex in yNta1 [50] (not shown here)). Nevertheless, Lnt seems to contain residues at similar positions mainly F416 and W415. F416A construct was expressed but could not rescue growth [3, 5]. W415A was also lethal, and W415 was designated as one of the putative phosphate binding residues (based on the bound chloride) [3], and for contacts with lipid 2.

#### Acknowledgements

T.E.A. is thankful to Science Foundation Ireland (SFI) for the personal Technology Innovation Development Award (TIDA).

#### References

- [1] G. Mao, Y. Zhao, X. Kang, Z. Li, Y. Zhang, X. Wang, F. Sun, K. Sankaran, X.C. Zhang, Crystal structure of *E. coli* lipoprotein diacylglycerol transferase, *Nat. Commun.* 7 (2016), 10198.
- [2] L. Vogeley, T. El Arnaout, J. Bailey, P.J. Stansfeld, C. Boland, M. Caffrey, Structural basis of lipoprotein signal peptidase II action and inhibition by the antibiotic globomycin, *Science* 351 (6275) (2016) 876–880.
- [3] C.L. Noland, M.D. Kattke, J. Diao, S.L. Gloor, H. Pantua, M. Reichelt, A.K. Katakam, D. Yan, J. Kang, I. Zilberleyb, M. Xu, S.B. Kapadia, J.M. Murray, Structural insights into



- lipoprotein N-acylation by *Escherichia coli* apolipoprotein N-acyltransferase, Proc. Natl. Acad. Sci. 114 (30) (2017) E6044–E6053.
- [4] M. Wiktor, D. Weichert, N. Howe, C.-Y. Huang, V. Olieric, C. Boland, J. Bailey, L. Vogeley, P.J. Stansfeld, N. Buddelmeijer, M. Wang, M. Caffrey, Structural insights into the mechanism of the membrane integral N-acyltransferase step in bacterial lipoprotein synthesis, Nat. Commun. 8 (2017), 15952.
- [5] G. Lu, Y. Xu, K. Zhang, Y. Xiong, H. Li, L. Cui, X. Wang, J. Lou, Y. Zhai, F. Sun, X.C. Zhang, Crystal structure of *E. coli* apolipoprotein N-acyl transferase, Nat. Commun. 8 (2017), 15948.
- [6] P.J. Stansfeld, J.E. Goose, M. Caffrey, E.P. Carpenter, J.L. Parker, S. Newstead, M.S.P. Sansom, MemProtMD: automated insertion of membrane protein structures into explicit lipid membranes, Structure 23 (7) (2015) 1350–1361, <https://doi.org/10.1016/j.str.2015.05.006>.
- [7] I.K. Dev, P.H. Ray, Rapid assay and purification of a unique signal peptidase that processes the prolipoprotein from *Escherichia coli* B, J. Biol. Chem. 259 (17) (1984) 11114–11120 <http://www.jbc.org/content/259/17/11114.full.pdf>.
- [8] M. Hussain, S. Ichihara, S. Mizushima, Accumulation of glyceride-containing precursor of the outer membrane lipoprotein in the cytoplasmic membrane of *Escherichia coli* treated with globomycin, J. Biol. Chem. 255 (8) (1980) 3707–3712.
- [9] M. Baumgartner, U. Karst, B. Gerstel, M. Loessner, J. Wehland, L. Jansch, Inactivation of Lgt allows systematic characterization of lipoproteins from *Listeria monocytogenes*, J. Bacteriol. 189 (2) (2007) 313–324.
- [10] H. Tjalsma, G. Zanen, G. Venema, S. Bron, J.M. van Dijk, The potential active site of the lipoprotein-specific (type II) signal peptidase of *Bacillus subtilis*, J. Biol. Chem. 274 (40) (1999) 28191–28197.
- [11] K. Becker, P. Sander, Mycobacterium tuberculosis lipoproteins in virulence and immunity – fighting with a double-edged sword, FEBS Lett. 590 (21) (2016) 3800–3819.
- [12] H. Antelmann, H. Tjalsma, B. Voigt, S. Ohlmeier, S. Bron, J.M. van Dijk, M. Hecker, A proteomic view on genome-based signal peptide predictions, Genome Res. 11 (9) (2001) 1484–1502.
- [13] H.C. Wu, Biosynthesis of lipoproteins, in: F.C. Neidhardt, R. Curtiss, J.L. Ingraham, E.C.C. Lin, K.B. Low, B. Magasanik, W.S. Reznikoff, M. Riley, M. Schaechter, H.E. Umberger (Eds.), *Escherichia coli* and Salmonella: Cellular and Molecular Biology, 2nd ed., vol. 1, ASM Press, Washington, D.C. 1996, pp. 1005–1014.
- [14] S.D. Gupta, W. Dowhan, H.C. Wu, Phosphatidylethanolamine is not essential for the N-acylation of apolipoprotein in *Escherichia coli*, J. Biol. Chem. 266 (15) (1991) 9983–9986.
- [15] A. Tschumi, C. Nai, Y. Auchli, P. Hunziker, P. Gehrig, P. Keller, T. Grau, P. Sander, Identification of apolipoprotein N-acyltransferase (Lnt) in mycobacteria, J. Biol. Chem. 284 (40) (2009) 27146–27156.
- [16] T. El Arnaout, Structure-Function Studies of the Prolipoprotein Signal Peptidase, LspA, Trinity College Dublin, 2013.
- [17] E.D. Lovullo, L.F. Wright, V. Isabella, J.F. Huntley, M.S. Pavelka, Revisiting the gram-negative lipoprotein paradigm, J. Bacteriol. 197 (10) (2015) 1705–1715.
- [18] M. Rezwani, T. Grau, A. Tschumi, P. Sander, Lipoprotein synthesis in mycobacteria, Microbiology 153 (3) (2007) 652–658.
- [19] J.K. Brülle, A. Tschumi, P. Sander, Lipoproteins of slow-growing mycobacteria carry three fatty acids and are N-acylated by apolipoprotein N-acyltransferase BCG\_2070c, BMC Microbiol. 13 (1) (2013) 223.
- [20] D.A. Widdick, M.G. Hicks, B.J. Thompson, A. Tschumi, G. Chandra, I.C. Sutcliffe, J.K. Brülle, P. Sander, T. Palmer, M.I. Hutchings, Dissecting the complete lipoprotein biogenesis pathway in *Streptomyces scabies*, Mol. Microbiol. 80 (5) (2011) 1395–1412.
- [21] N. Mohiman, M. Argenti, S.M. Batt, D. Cornu, M. Masi, L. Eggeling, G. Besra, N. Bayan, The ppm operon is essential for acylation and glycosylation of lipoproteins in *Corynebacterium glutamicum*, PLoS One 7 (9) (2012), e46225.
- [22] J.K. Brülle, T. Grau, A. Tschumi, Y. Auchli, R. Burri, S. Polsfuss, P.M. Keller, P. Hunziker, P. Sander, Cloning, expression and characterization of *Mycobacterium tuberculosis* lipoprotein LprF, Biochem. Biophys. Res. Commun. 391 (1) (2010) 679–684.
- [23] K. Kurokawa, H. Lee, K.B. Roh, M. Asanuma, Y.S. Kim, H. Nakayama, A. Shiratsuchi, Y. Choi, O. Takeuchi, H.J. Kang, N. Dohmae, Y. Nakanishi, S. Akira, K. Sekimizu, B.L. Lee, The triacylated ATP binding cluster transporter substrate-binding lipoprotein of *Staphylococcus aureus* functions as a native ligand for toll-like receptor 2, J. Biol. Chem. 284 (13) (2009) 8406–8411.
- [24] M. Asanuma, K. Kurokawa, R. Ichikawa, K.H. Ryu, J.H. Chae, N. Dohmae, B.L. Lee, H. Nakayama, Structural evidence of alpha-aminoacylated lipoproteins of *Staphylococcus aureus*, FEBS J. 278 (5) (2011) 716–728.
- [25] K.M. Armbruster, T.C. Meredith, Identification of the lyso-form N-acyl intramolecular transferase in low-GC firmicutes, J. Bacteriol. 199 (11) (2017).
- [26] K. Kurokawa, K.H. Ryu, R. Ichikawa, A. Masuda, M.S. Kim, H. Lee, J.H. Chae, T. Shimizu, T. Saitoh, K. Kuwano, S. Akira, N. Dohmae, H. Nakayama, B.L. Lee, Novel bacterial lipoprotein structures conserved in low-GC content gram-positive bacteria are recognized by toll-like receptor 2, J. Biol. Chem. 287 (16) (2012) 13170–13181.
- [27] L.-T. Ruan, R.-C. Zheng, Y.-G. Zheng, Y.-C. Shen, Purification and characterization of R-stereospecific amidase from *Brevibacterium epidermidis* ZJB-07021, Int. J. Biol. Macromol. 86 (2016) 893–900.
- [28] H.C. Pace, C. Brenner, The nitrilase superfamily: classification, structure and function, Genome Biol. 2 (1) (2001) (REVIEWS0001).
- [29] H. Hashemi Gahruei, M. Niakousari, Antioxidant, antimicrobial, cell viability and enzymatic inhibitory of antioxidant polymers as biological macromolecules, Int. J. Biol. Macromol. 104 (2017) 606–617.
- [30] C.L. Hung, J.H. Liu, W.C. Chiu, S.W. Huang, J.K. Hwang, W.C. Wang, Crystal structure of *Helicobacter pylori* formamidase AmiF reveals a cysteine-glutamate-lysine catalytic triad, J. Biol. Chem. 282 (16) (2007) 12220–12229.
- [31] B.W. Weber, S.W. Kimani, A. Varsani, D.A. Cowan, R. Hunter, G.A. Venter, J.C. Gumbart, B.T. Sewell, The mechanism of the amidases: mutating the glutamate adjacent to the catalytic triad inactivates the enzyme due to substrate mispositioning, J. Biol. Chem. 288 (40) (2013) 28514–28523.
- [32] J.E. Raczynska, C.E. Vorgias, G. Antranikian, W. Rypniewski, Crystallographic analysis of a thermoactive nitrilase, J. Struct. Biol. 173 (2) (2011) 294–302.
- [33] J. Andrade, A. Karmali, M.A. Carrondo, C. Frazao, Structure of amidase from *Pseudomonas aeruginosa* showing a trapped acyl transfer reaction intermediate state, J. Biol. Chem. 282 (27) (2007) 19598–19605.
- [34] J. Prava, P. G. A. Pan, Functional assignment for essential hypothetical proteins of *Staphylococcus aureus* N315, Int. J. Biol. Macromol. 108 (2018) 765–774.
- [35] B.C. Jennings, M.E. Linder, DHHC protein S-acyltransferases use similar ping-pong kinetic mechanisms but display different acyl-CoA specificities, J. Biol. Chem. 287 (10) (2012) 7236–7245.
- [36] D.A. Mitchell, G. Mitchell, Y. Ling, C. Budde, R.J. Deschenes, Mutational analysis of *Saccharomyces cerevisiae* Erf2 reveals a two-step reaction mechanism for protein palmitoylation by DHHC enzymes, J. Biol. Chem. 285 (49) (2010) 38104–38114.
- [37] M.S. Rana, P. Kumar, C.J. Lee, R. Verardi, K.R. Rajashankar, A. Banerjee, Fatty acyl recognition and transfer by an integral membrane S-acyltransferase, Science 359 (6372) (2018).
- [38] R.M. Robertson, J. Yao, S. Gajewski, G. Kumar, E.W. Martin, C.O. Rock, S.W. White, A two-helix motif positions the lysophosphatidic acid acyltransferase active site for catalysis within the membrane bilayer, Nat. Struct. Mol. Biol. 24 (8) (2017) 666–671.
- [39] T. Nakai, T. Hasegawa, E. Yamashita, M. Yamamoto, T. Kumasaka, T. Ueki, H. Nanba, Y. Ikenaka, S. Takahashi, M. Sato, T. Tsukihara, Crystal structure of N-carbamyl-D-amino acid amidohydrolase with a novel catalytic framework common to amidohydrolases, Structure 8 (7) (2000) 729–738.
- [40] D. Vidal-Ingigliardi, S. Lewenza, N. Buddelmeijer, Identification of essential residues in apolipoprotein N-acyl transferase, a member of the CN hydrolase family, J. Bacteriol. 189 (12) (2007) 4456–4464.
- [41] C. Robichon, D. Vidal-Ingigliardi, A.P. Pugsley, Depletion of apolipoprotein N-acyltransferase causes mislocalization of outer membrane lipoproteins in *Escherichia coli*, J. Biol. Chem. 280 (2) (2005) 974–983.
- [42] Y. Zhang, J. Skolnick, Scoring function for automated assessment of protein structure template quality, Proteins: Structure, Function, and Bioinformatics 57 (4) (2004) 702–710.
- [43] N. Buddelmeijer, R. Young, The essential *Escherichia coli* apolipoprotein N-acyltransferase (Lnt) exists as an extracytoplasmic thioester acyl-enzyme intermediate, Biochemistry 49 (2) (2010) 341–346.
- [44] A.C. Wallace, R.A. Laskowski, J.M. Thornton, LIGPLOT: a program to generate schematic diagrams of protein-ligand interactions, Protein Eng. 8 (2) (1995) 127–134.
- [45] S. Gelis-Jeanvoine, S. Lory, J. Oberto, N. Buddelmeijer, Residues located on membrane-embedded flexible loops are essential for the second step of the apolipoprotein N-acyltransferase reaction, Mol. Microbiol. 95 (4) (2015) 692–705.
- [46] O.B. Clarke, D. Tomasek, C.D. Jorge, M.B. Dufresne, M. Kim, S. Banerjee, K.R. Rajashankar, L. Shapiro, W.A. Hendrickson, H. Santos, F. Mancia, Structural basis for phosphatidylinositol-phosphate biosynthesis, Nat. Commun. 6 (2015) 8505.
- [47] Z.-Q. Liu, M.-M. Lu, X.-H. Zhang, F. Cheng, J.-M. Xu, Y.-P. Xue, L.-Q. Jin, Y.-S. Wang, Y.-G. Zheng, Significant improvement of the nitrilase activity by semi-rational protein engineering and its application in the production of iminodiacetic acid, Int. J. Biol. Macromol. 116 (2018) 563–571.
- [48] V. Kumar, V. Kumar, T.C. Bhalla, Alkaline active cyanide dihydratase of *Flavobacterium indicum* MTCC 6936: growth optimization, purification, characterization and in silico analysis, Int. J. Biol. Macromol. 116 (2018) 591–598.
- [49] H. Liu, Y. Gao, M. Zhang, X. Qiu, A.J. Cooper, L. Niu, M. Teng, Structures of enzyme-intermediate complexes of yeast Nit2: insights into its catalytic mechanism and different substrate specificity compared with mammalian Nit2, Acta Crystallogr. D Biol. Crystallogr. 69 (Pt 8) (2013) 1470–1481.
- [50] M.K. Kim, J. Oh, B.G. Lee, H.K. Song, Structural basis for dual specificity of yeast N-terminal amidase in the N-end rule pathway, Proc. Natl. Acad. Sci. U. S. A. 113 (44) (2016) 12438–12443.